BIOCHEMISTRY
including biophysical chemistry & molecular biology

Article

pubs.acs.org/biochemistry

Human Serum Transferrin: Is There a Link among Autism, High Oxalate Levels, and Iron Deficiency Anemia?

Ashley N. Luck,[†,§] Cedric E. Bobst,[‡] Igor A. Kaltashov,[‡] and Anne B. Mason*[,†]

[†]Department of Biochemistry, University of Vermont, College of Medicine, 89 Beaumont Avenue, Burlington, Vermont 05405, United States

[‡]Department of Chemistry, University of Massachusetts at Amherst, Amherst, Massachusetts 01003, United States

Supporting Information

ABSTRACT: It has been previously suggested that large amounts of oxalate in plasma could play a role in autism by binding to the bilobal iron transport protein transferrin (hTF), thereby interfering with iron metabolism by inhibiting the delivery of iron to cells. By examining the effect of the substitution of oxalate for the physiologically utilized synergistic carbonate anion in each lobe of hTF, we sought to provide a molecular basis for or against such a role. Our work clearly shows both qualitatively (6 M urea gels) and quantitatively (kinetic analysis by stopped-flow spectrofluorimetry) that the presence of oxalate in place of carbonate in each binding site of hTF does indeed greatly interfere with the removal of iron from each lobe (in the absence and presence of the specific hTF receptor). However, we also clearly demonstrate that once the iron is bound within each lobe of hTF, neither anion can displace the other. Additionally, as verified by urea gels and electrospray mass spectrometry, formation of completely homogeneous hTF−anion complexes requires that all iron must first be removed and hTF then reloaded with iron in the presence of either carbonate or oxalate. Significantly, experiments described here show that carbonate is the preferred binding partner; i.e., even if an equal amount of each anion is available during the iron loading process, the hTF−carbonate complex is formed.

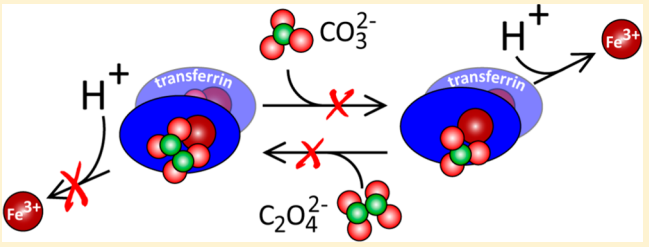

Autism spectrum disorders (ASD) are complex neurological/developmental disorders that severely impact the social, behavioral, and communication skills of affected children. Recent findings from the Centers for Disease Control and Prevention suggest that as many as 1 in 88 children may be affected with some form of ASD.[1] Despite the increasing frequency of diagnosis and numerous suggestions and/or theories about the origin(s) of this apparent sudden epidemic of ASD, no single cause has been identified. In fact, it seems most likely that multiple genetic and environmental factors are involved in the pathology of ASD.[2−5]

Interestingly, along with the typical behavioral and communication issues, gastrointestinal symptoms often exist in children with ASD.[6,7] This observation could indicate that a more complex and global metabolic disorder exists. Obviously, at least some of the same metabolic imbalances in children with ASD could be related to, or responsible for, the observed impairment of cognitive development and function.

More recently, largely anecdotal evidence suggests that the metabolism and homeostasis of oxalate may be a factor in ASD. Providing some scientific support for the involvement of oxalate in ASD is a study showing that children with ASD displayed a plasma level of oxalate increased 3-fold compared to those of age- and gender-matched controls.[7] Nevertheless, the precise molecular origin and potential effect of hyperoxalemia in children with ASD remain unclear. Given these findings, it is imperative to provide a more solid scientific basis, either for or against, a possible role of oxalate in ASD because information currently available on the Internet touts the benefits of a low-oxalate diet to improve the cognitive function and behavior of children with ASD.

Oxalate ($C_2O_4^{2-}$) is a relatively simple molecule that, when in complex with divalent metallic cations such as Ca^{2+}, forms insoluble crystals that eventually can result in kidney stones. Oxalate is acquired by the body through dietary intake (various foods, especially plant materials, including grains, seeds, nuts, vegetables such as chard, beet roots, and spinach, and various fruits such as rhubarb, are high in oxalate). Additionally, oxalate is also produced within the body[8,9] as the final degradation product of a number of amino acids (including the aromatic amino acids tyrosine, phenylalanine, and tryptophan) and also ascorbate.

In addition to the single report on hyperoxalemia,[7] a number of studies outside the United States have highlighted the increased prevalence of iron deficiency (ID) and/or iron deficiency anemia (IDA) in children with ASD in comparison to age-matched controls.[10−13] However, this finding was not confirmed in a recent study of children with ASD in the United

Received: August 28, 2013
Revised: October 21, 2013
Published: October 23, 2013

   dx.doi.org/10.1021/bi401190m | *Biochemistry* 2013, 52, 8333−8341

States.[14] Of interest, a small subset of children with ASD and ID/IDA also appeared to be nonresponsive to oral iron therapy;[15] i.e., the ID/IDA was iron-refractory. It is well established that iron is critical to many essential biological processes, including oxygen and electron transport,[16] and that it exerts both positive and negative effects on brain function.[17−19] Therefore, ID/IDA could possibly contribute to the adverse effects on cognitive development and function observed in children with ASD.

Intriguingly, it is possible that these seemingly unrelated metabolic imbalances (gastrointestinal dysfunction, hyperoxalemia, and IDA) might be connected. With the task of binding iron (in the form of Fe^{3+}) and safely delivering it to cells, the bilobal glycoprotein human serum transferrin (hTF) comprises the most dynamic iron pool within the human body, turning over nearly 10 times per day.[20] Following production of hTF in the liver and secretion into the blood, each lobe (termed the N- and C-lobes) binds Fe^{3+} very tightly ($K_d \sim 10^{22}$ M^{-1}), yet reversibly.[21] Two tyrosine residues, one aspartic acid, and one histidine residue (Tyr95, Tyr188, Asp63, and His249 in the N-lobe and Tyr426, Tyr517, Asp392, and His585 in the C-lobe, respectively) coordinate the Fe^{3+} in each lobe of hTF. The distorted octahedral coordination of the iron is completed by the final two ligands provided by a synergistic anion. With its relatively high concentration in serum, bicarbonate/carbonate (HCO_3^{2-}/CO_3^{2-}) was originally suggested and has since been confirmed by a number of X-ray crystallographic structures to serve as the physiologically relevant synergistic anion.[22,23] The crystal structures further revealed that the synergistic carbonate is anchored by a conserved hTF residue (Arg124 in the N-lobe and Arg456 in the C-lobe). As its name implies, a suitable synergistic anion is an absolute requirement for high-affinity Fe^{3+} binding by hTF within the binding cleft of each lobe.[24] Consistent with the dynamic nature of many proteins in solution,[25] equilibrium probably exists between the open and closed cleft in each lobe of hTF.[26] It has also been suggested that the synergistic anion may bind first to preform the binding site,[27,28] because as indicated by the residue numbers above, the iron binding residues are distant in the primary sequence. Thus, high-affinity binding of iron occurs when a suitable synergistic anion and ferric iron are present to drive the equilibrium toward the fully iron-bound closed conformation.

At the neutral pH of ∼7.4 of the blood, iron-bearing hTF binds with nanomolar affinity to the transferrin receptor (TFR), located on the cell surface of all iron-requiring, i.e., actively dividing, cells. The hTF−TFR complex enters the cell via clathrin-dependent endocytosis.[29] An ATP-dependent H^+ pump lowers the pH within the endosome where salt and an unidentified chelator initiate the TFR-mediated release of iron from hTF.[30] At endosomal pH, apohTF remains tightly bound to the TFR. Return of the apohTF−TFR complex to the cell surface initiates the release of apohTF into the blood (pH 7.4), where it can bind more Fe^{3+}. Importantly, removal of Fe^{3+} from hTF in solution requires a decrease in pH (from 7.4 to <6.0) to protonate the synergistic anion as well as pH-sensitive "second-shell" residues. These residues do not directly coordinate the Fe^{3+} but form hydrogen bonds with the primary iron-binding ligands and are involved in the mechanism of release of iron from each lobe.[31−33] In the N-lobe, Lys206 and Lys296 on opposite sides of the binding cleft share a hydrogen bond when Fe^{3+} is bound.[34] In response to low pH, protonation causes repulsion of these lysine residues, triggering cleft opening and allowing iron release. A triad of amino acid residues occupies equivalent positions in the C-lobe.[34] Lys534 (corresponding to Lys206 in the N-lobe) is located across the binding cleft from Arg632 (equivalent to Lys296 in the N-lobe) in the C1 subdomain. Similar to the dilysine trigger in the N-lobe, it has been suggested that Lys534 may share a hydrogen bond with Arg632.[34] The triad is completed by Asp634, which has been shown to stabilize the interaction of Lys534 and Arg632.[35] The role of these residues in the mechanism of iron release has been confirmed by mutagenesis studies.[32,33] In fact, substitution of Lys206 in the N-lobe with glutamate or substitution of Lys534 or Arg632 with alanine has allowed the creation of hTF constructs in which the iron is literally locked in the cleft.[36]

As reported nearly 40 years ago, oxalate ($C_2O_4^{2-}$) can substitute for carbonate to promote high-affinity binding of Fe^{3+} to hTF.[37] Previous findings from our laboratory indicate that when oxalate serves as the synergistic anion within the isolated N-lobe of recombinant hTF [$hTF/2N_{(OX)}$], iron release is much slower and requires a lower pH.[38] Additionally, full-length hTF with oxalate bound as the synergistic anion [$hTF_{(OX)}$] completely prevents the delivery of iron to HeLa cells.[38] The lower pK_a of oxalate (4.2) compared to that of carbonate (6.4) allowed us to rationalize these results. Moreover, on the basis of the 1.2 Å crystal structure of $hTF/2N_{(OX)}$, oxalate binds within the iron-binding cleft in a bidentate manner, providing nearly perfect symmetry and further stabilizing its resistance to protonation in comparison to the more vulnerable carbonate anion.[38]

The reports that (1) plasma oxalate levels in children with ASD tend to be high,[7] (2) the prevalence of iron-refractory ID/IDA in children with ASD is high,[10−13,15] (3) children with ASD have gastrointestinal problems that could affect the uptake of both iron and oxalate in the gut,[6] and (4) $hTF/2N_{(OX)}$ and Fe_2 $hTF_{(OX)}$ do not readily relinquish iron[38] collectively suggest a potential link between oxalate and iron deficiency anemia in autism. Thus, high plasma oxalate levels and iron-refractory ID/IDA in children with ASD might be mediated via $hTF_{(OX)}$. Therefore, in this study, we set out to investigate the hypothesis that hTF provides a crucial link between high plasma oxalate levels and iron deficiency in children with ASD. First, we quantitatively examined the iron release properties of diferric hTF and the two monoferric hTFs with oxalate bound as the synergistic anion using standardized methods and recombinant hTF that we have developed over the past several years.[35] We then evaluated whether the two synergistic anions (carbonate and oxalate) were able to displace and/or compete with one another at physiologically relevant concentrations of each. This is critical to determining the possible relevance of a high oxalate level as a causative agent of IDA in children with ASD (if it exists). Finally, we further characterized the oxalate-containing hTF samples by mass spectrometry analysis on a high-resolution instrument.

MATERIALS AND METHODS

Materials. Dulbecco's modified Eagle's medium-Ham F-12 nutrient mixture (DMEM-F12) and fetal bovine serum (FBS) were obtained from the GIBCO-BRL Life Technologies Division of Invitrogen. Antibiotic-antimycotic solution (100×) and trypsin were from Mediatech, Inc. Both Pro293A-CDM serum-free medium and L-glutamine were purchased from Lonza. All tissue culture dishes, flasks, and Corning expanded surface roller bottles were obtained from local distributors. Ultracel 30 kDa molecular weight cutoff (MWCO) membrane microconcentrator devices were manufactured by Amicon. Ni-

dx.doi.org/10.1021/bi401190m | Biochemistry 2013, 52, 8333−8341

nitrilotriacetic acid (NTA) resin was from Qiagen. Hi-prep 26/60 Sephacryl S-200HR and S-300HR columns were acquired from GE Healthcare. Ethylenediaminetetraacetic acid (EDTA) was from Fisher. NTA, $K_2C_2O_4·H_2O$, and ferrous ammonium sulfate were from Sigma (St. Louis, MO). Novex 6% tris(hydroxymethyl)aminomethane/borate/EDTA (TBE)−urea mini-gels, TBE running buffer (5×), and TBE−urea sample buffer (2×) were from Invitrogen.

Expression and Purification of hTFs and the Soluble Portion of the TFR (sTFR). The expression and purification of baby hamster kidney (BHK) cell-derived recombinant NHis-tagged hTF (diferric hTF, Fe_2hTF; Fe_NhTF, monoferric N-lobe hTF in which mutation of iron binding ligands, Y426F and Y517F, prevents iron binding in the C-lobe; Fe_ChTF, monoferric C-lobe hTF in which mutation of iron binding ligands, Y95F and Y188F, prevents iron binding in the N-lobe) have been previously described.[39] The K206E mutation,[31,32,36] which prevents the release of iron from the N-lobe, as well as the Lys534[32]and Arg632 mutations,[32,36] which prevent the release of iron from the C-lobe, have also been previously reported. To ensure iron saturation and stabilize the recombinant hTF, ferric iron (in the form of Fe^{3+}-NTA) was added to collected tissue culture medium prior to purification. The Fe-NTA solution was prepared by mixing an appropriate amount of 25 mM ferrous ammonium sulfate (in 0.01 N HCl) with 100 mM NTA to obtain an Fe:NTA ratio of 1:2. Collected medium was reduced in volume using a tangential flow device with a 30 kDa MWCO membrane and partially exchanged into 5 mM Tris-HCl buffer (pH 8.0) containing 0.02% sodium azide. Following cotton filtration and/or centrifugation to remove any cellular debris (6000*g* for 15 min), 5× Qiagen start buffer was added to the supernatant to yield a final concentration of 1× Qiagen start buffer [50 mM Tris-HCl (pH 7.5), 300 mM NaCl, 20 mM imidazole, 10% glycerol, and 0.05% sodium azide]. The hTF was then captured by being passed over a Qiagen Ni-NTA column (8 mL of resin, 2 mL/min) and eluted by the addition of 250 mM imidazole to the 1× Qiagen start buffer. Pooled fractions were concentrated using 30 kDa MWCO Ultracel microconcentrators, and final purification was accomplished by passage over a Sephacryl S-200 HR gel filtration column in 100 mM NH_4HCO_3. Pooled fractions of purified carbonate containing hTF were concentrated to 15 mg/mL using a 30 kDa MWCO Ultracel microconcentrator.

The production and purification of the His-tagged sTFR consisting of residues 121−760 were also conducted as previously described.[40]

hTF−sTFR Complex Formation and Purification. The hTF−sTFR complexes were prepared by adding a small molar excess (∼20%) of hTF to 1.5 mg of each mutant sTFR. Following equilibration at room temperature for ∼5 min, hTF−mutant sTFR complexes were purified by being passed over a Sephacryl S300HR gel filtration column in 100 mM NH_4HCO_3 to remove excess hTF. Fractions containing the complex were concentrated to 15 mg/mL with respect to hTF.

$hTF_{(OX)}$ Formation. Oxalate-containing samples were prepared by two different methods as follows. In the first method, carbonate-containing hTF (Fe_2hTF, Fe_NhTF, and Fe_ChTF) or hTF−sTFR complexes were exchanged into 200 mM $K_2C_2O_4·H_2O$ using microconcentrators (30 kDa MWCO). After incubation (3−4 days at 4 °C) in 200 mM $K_2C_2O_4·H_2O$, additional Fe-NTA was added to the hTF samples to ensure complete iron saturation. Samples were then exchanged into 200 mM $K_2C_2O_4·H_2O$ to remove excess Fe-NTA. In the second method, apohTF was produced by incubating the hTF samples (Fe_2hTF, Fe_NhTF, and Fe_ChTF) in 500 mM sodium acetate (pH 4.9) containing 1 mM NTA and 1 mM EDTA overnight at 4 °C. Following an exchange into 100 mM KCl, the apo samples were then exchanged into 200 mM $K_2C_2O_4·H_2O$ before an excess amount of iron (in the form of ferrous sulfate) was added.

Analysis by ESI-MS. Samples prepared as described above were exhaustively exchanged into 50 mM ammonium acetate (pH 6.7) on microconcentrators (30 kDa MWCO) and adjusted to a final protein concentration of 5 μM. Mass spectra were recorded on a solariX (Bruker Daltonics, Billerica, MA) 7T FT-ICR instrument with collisional energy parameters in the source kept at minimal values to preserve ligand−protein complexes in the gas state. Ligand binding was disrupted by adding a solution of formic acid to lower the sample pH to 3.7 and incubation for 15 min at 25 °C. All spectra consist of 500 averaged scans collected over a total acquisition time of 6 min. External calibration from m/z 2000 to 5000 was performed using sodium perfluoroheptonate clusters.

Urea Gel Analysis. The iron status of hTF and hTF−sTFR complexes was evaluated by urea gel electrophoresis using Novex 6% TBE−urea mini gels in 90 mM Tris-borate (pH 8.4) containing 16 mM EDTA as previously described.[36,41] Iron-containing complexes were mixed in a 1:1 ratio with 2× TBE−urea gel sample buffer (final concentration of 0.5 μg/μL). To determine the extent of iron removal, an aliquot of each sample was added to iron removal buffer [100 mM MES buffer (pH 5.6) containing 300 mM KCl and 4 mM EDTA] and incubated at room temperature for 5 min. The iron removal process was halted by addition of 2× TBE−urea gel sample buffer. Samples (2.5 μg) were loaded, and the gel was electrophoresed for 2.25 h at 125 V. Protein bands were visualized by being stained with Coomassie blue.[42]

Kinetic Analysis of the Release of Iron from hTF with or without sTFR at pH 5.6. The release of iron from hTF mutants, $hTF_{(OX)}$, hTF mutants, and $hTF_{(OX)}$ complexes was monitored at 25 °C as previously described using an Applied Photophysics SX.20MV stopped-flow spectrofluorimeter.[36] The contents of one syringe [hTF sample or hTF−sTFR complex (375 nM) in 300 mM KCl] were rapidly mixed with the iron removal buffer in the second syringe, MES buffer (200 mM, pH 5.6), KCl (300 mM), and EDTA (8 mM). Rate constants were determined by fitting the change in fluorescence intensity versus time using Origin (version 7.5) to standard models as described in detail previously.[36] All data were corrected to zero fluorescence intensity at time zero before fitting.

Displacement of Carbonate by Oxalate. Carbonate-containing Fe_2hTF in 25 mM NH_4HCO_3 was incubated with increasing concentrations of $K_2C_2O_4·H_2O$ (0−50 μM) for 2 h at 37 °C. Samples (2.5 μg) were removed and exposed to iron removal buffer [100 mM MES buffer (pH 5.6) containing 300 mM KCl and 4 mM EDTA] and incubated at room temperature for 15 min. The iron removal process was halted by addition of 2× TBE−urea gel sample buffer, and samples (2.5 μg) were run and visualized as described above.

Displacement of Oxalate by Carbonate. Oxalate-containing $Fe_2hTF_{(OX)}$ in increasing concentrations of $K_2C_2O_4·H_2O$ (0−50 μM) was incubated with 25 mM NH_4HCO_3 for 2 h at 37 °C. Samples (2.5 μg) were removed and exposed to iron removal buffer [100 mM MES buffer (pH 5.6) containing 300 mM KCl and 4 mM EDTA] and incubated

dx.doi.org/10.1021/bi401190m | *Biochemistry* 2013, 52, 8333−8341

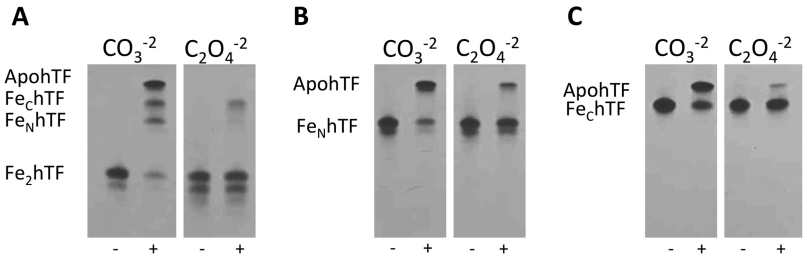

Figure 1. Urea gel analysis of carbonate (CO_3^{2-})- and oxalate ($C_2O_4^{2-}$)-containing Fe_2hTF (A), Fe_NhTF (B), and Fe_ChTF (C). Samples were electrophoresed before and after (+) incubation with iron removal buffer [100 mM MES (pH 5.6) containing 300 mM KCl and 4 mM EDTA] for 15 min.

at room temperature for 15 min. The iron removal process was halted by addition of 2× TBE−urea gel sample buffer, and samples (2.5 μg) were run and visualized as described above.

Competitive Synergistic Anion Binding to ApohTF. ApohTF was produced by incubating Fe_2hTF in 500 mM sodium acetate (pH 4.9) containing 1 mM NTA and 1 mM EDTA overnight at 4 °C followed by extensive exchange into 100 mM KCl. ApohTF in 100 mM KCl (final concentration of 5 mM) was incubated with 25 mM NH_4HCO_3 containing increasing concentrations of $K_2C_2O_4{\cdot}H_2O$ (0−50 μM) and excess Fe-NTA for 2 h at 37 °C. Samples (2.5 μg) were removed and exposed to iron removal buffer [100 mM MES buffer (pH 5.6) containing 300 mM KCl and 4 mM EDTA] and incubated at room temperature for 15 min. The iron removal process was halted by addition of 2× TBE−urea gel sample buffer, and samples (2.5 μg) were run and visualized as described above.

RESULTS AND DISCUSSION

Effect of Oxalate on the Release of Iron from hTF. The results of a qualitative evaluation (by 6% TBE−urea gels) of the release of iron from various hTF and $hTF_{(OX)}$ constructs are presented in Figure 1. In comparison to the respective carbonate control, the presence of oxalate in the three hTF constructs significantly decreases the amount of iron that is released within the tested time frame. Although in this format a small amount of iron remains bound in each lobe of the diferric control (i.e., both monoferric hTF species are present), after a 15 min treatment with our standard iron removal buffer [100 mM MES (pH 5.6) containing 300 mM KCl and 4 mM EDTA], very little Fe_2hTF remains (Figure 1A). Under identical conditions, it appears that a small amount of Fe^{3+} is removed from the N-lobe [as indicated by the presence of $Fe_ChTF_{(OX)}$]; however, most of the $Fe_2hTF_{(OX)}$ sample remains in the diferric state. Treatment of $Fe_NhTF_{(OX)}$ and $Fe_ChTF_{(OX)}$ with our iron removal regimen also results in far less iron removal compared to that seen for the carbonate control samples (Figure 1B,C). To provide a basis for comparison, we have included the results of the same experiment with our $Lock_N$−$Lock_C$hTF constructs in which both lobes are compromised by substitution of key residues that help to trigger iron release (Lys206 in the N-lobe and Lys534 and Arg632 in the C-lobe).[32,33,36] As clearly shown in Figure S1 of the Supporting Information, these constructs are extremely resistant to iron removal under the conditions used. In fact, only the K206E/K534E Fe_2hTF mutant releases any iron, apparently from the C-lobe, because the migration of the band corresponds to Fe_NhTF.

We are able to provide a far more quantitative estimate of the dramatic decrease in the rate of release of iron from the $hTF_{(OX)}$ samples from kinetic rate constants obtained by fitting the increase in the intrinsic tryptophan fluorescence of hTF as Fe^{3+} is released. Although as clearly shown in the urea gel analysis, very little iron is released from the $hTF_{(OX)}$ constructs, a small increase in the intrinsic tryptophan fluorescence was observed under our standard iron removal conditions in the stopped-flow format. In contrast to the respective controls, which yield either two or three rate constants assigned to iron release and conformational events,[35,36] all of the oxalate samples fit to a simple A → B model (Table 1) and yielded

Table 1. Kinetic Rate Constants for the Release of Iron from $hTF_{(OX)}$ Samples

construct	k_1 (min^{-1})	k_2 (min^{-1})	k_3 (min^{-1})
Fe_2hTF^a	17.7 ± 2.2 (k_N)	0.65 ± 0.06 (k_C)	
$Fe_2hTF_{(OX)}$	–	0.29 ± 0.01	
construct	k_1 (min^{-1})	k_2 (min^{-1})	k_3 (min^{-1})
Fe_NhTF^a	24.8 ± 3.2 (k_N)	5.8 ± 1.2	1.1 ± 0.1
$Fe_NhTF_{(OX)}$	–	–	0.37 ± 0.01
construct	k_1 (min^{-1})	k_2 (min^{-1})	
Fe_ChTF^a	0.79 ± 0.11 (k_C)	1.9 ± 0.5	
$Fe_ChTF_{(OX)}$	–	0.30 ± 0.01	

[a]From ref 36. See Figure S4 of the Supporting Information for iron-dependent changes as a function of time and the fit of this kinetic data to yield the rate constants in this table.

a single very slow kinetic rate constant that we assign to an unknown pH-induced conformational event. As an additional control, an increase in the intrinsic tryptophan fluorescence is observed in the $Lock_N$−$Lock_C$hTF constructs, which also do not release iron upon being exposed to low pH. As shown in Table S1 of the Supporting Information, three of the four $Lock_N$−$Lock_C$hTF constructs fit to a more complex A → B → C model than the $hTF_{(OX)}$ constructs. Noting the unusually large 95% confidence intervals obtained with the locked constructs, we found the first rate (k_1) is similar to the rate constant obtained from the $hTF_{(OX)}$ constructs (Table S1 of the Supporting Information vs Table 1). Interestingly, the second rate (k_2) of these $Lock_N$−$Lock_C$hTF constructs is very slow and additionally is the only rate obtained for the (K206E/R632A Fe_2hTF) $Lock_N$−$Lock_C$hTF construct (Table S1 of the Supporting Information). Given the drastically slowed rate constants and the fact that little iron is removed from any of the $Lock_N$−$Lock_C$hTF constructs or $hTF_{(OX)}$ samples, these very slow rates are assigned to small pH-induced conformational events. Collectively, it is very clear from the kinetic evaluation (by both urea gel and intrinsic tryptophan fluorescence) that little or no iron is removed from either the oxalate-containing hTF samples or the $Lock_N$−$Lock_C$hTF constructs.

dx.doi.org/10.1021/bi401190m | Biochemistry 2013, 52, 8333−8341

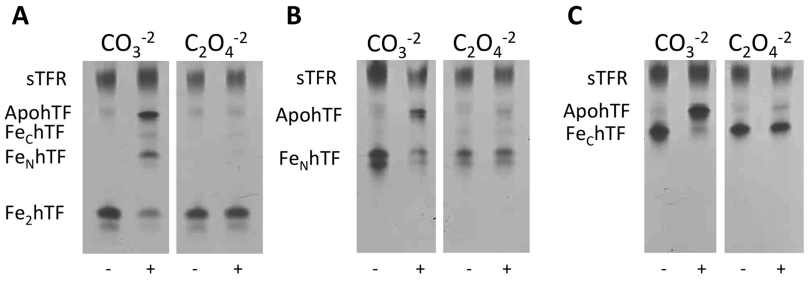

Figure 2. Urea gel analysis of carbonate (CO_3^{2-})- and oxalate ($C_2O_4^{2-}$)-containing Fe_2hTF–sTFR (A), Fe_NhTF–sTFR (B), and Fe_ChTF–sTFR (C) complexes. Samples were electrophoresed before and after (+) incubation with iron removal buffer [100 mM MES (pH 5.6) containing 300 mM KCl and 4 mM EDTA] for 5 min.

Effect of Oxalate on the Release of Iron from hTF–sTFR Complexes. To determine whether the substitution of oxalate as the synergistic anion affected the removal of iron from hTF–sTFR complexes, the $hTF_{(OX)}$–sTFR complexes were electrophoresed on a urea gel after a 5 min incubation in our standard iron removal buffer (pH 5.6). As reported previously, the sTFR significantly impacts the kinetics and mechanism of release of iron from each lobe of hTF.[36,41,43−45] Specifically, when the sample is bound to the soluble portion of the TFR, the rate of release of iron from the C-lobe is increased and the rate of release of iron from the N-lobe is decreased, making the two rates more equivalent.[35,36] As clearly shown in Figure 2, the release of iron from hTF is almost entirely inhibited when oxalate serves as the synergistic anion in the hTF–sTFR complexes. As expected, these results are replicated in three of the four $Lock_N$–$Lock_C$hTF–sTFR complexes (Figure S2 of the Supporting Information), which release very little, if any, iron even after a 15 min incubation in our standard iron removal buffer. Interestingly, the K534E mutation does not appear to completely lock Fe^{3+} in the C-lobe in the presence of the sTFR, as indicated by observation of a band corresponding to Fe_NhTF in the K206E/K534E Fe_2hTF–sTFR complex (Figure S2 of the Supporting Information).

The dramatic decrease in the rate of release of iron from the oxalate samples is further validated by the kinetic rate constants obtained from fitting the increase in intrinsic tryptophan fluorescence after exposing the $hTF_{(OX)}$–sTFR complexes to our "endosomal" conditions (Table 2). While the conformational change preceding the release of iron from the Fe_ChTF–sTFR complex (k_1) is maintained in the $Fe_ChTF_{(OX)}$–sTFR complex, a similar conformational change is lost in the $Fe_NhTF_{(OX)}$–sTFR complex in comparison to the Fe_NhTF–sTFR control. Additionally, a similar rate constant is obtained from the fitting of one of the $Lock_N$–$Lock_C$hTF complexes [K206E/R632E Fe_2hTF–sTFR (Table S2 of the Supporting Information)]. All the $hTF_{(OX)}$–sTFR complexes give rise to a similar rate constant [$k \approx 0.6$ min^{-1} (Table 2)] that is slower than any of the rates obtained for the four $Lock_N$–$Lock_C$hTF constructs (Table S2 of the Supporting Information). Intriguingly, the $Fe_2hTF_{(OX)}$–sTFR complex fits to an A → B → C model where $k_1 = k_2$ [$k = 0.6$ min^{-1} (Table 2)]. Because very little if any Fe^{3+} is removed from the $Fe_2hTF_{(OX)}$–sTFR complex, the actual events to which these two kinetic rate constants correspond remain unclear but could potentially be the combination of rates observed for the $Fe_NhTF_{(OX)}$–sTFR and $Fe_ChTF_{(OX)}$–sTFR complexes (Table 2). We conclude that the sTFR is unable to overcome either the presence of oxalate as the synergistic anion or the effect of the mutations in the $Lock_N$–$Lock_C$hTF constructs as very little iron can be released from these hTF–sTFR complexes.

Table 2. Kinetic Rate Constants for the Release of Iron from $hTF_{(OX)}$–sTFR Complexes

hTF–sTFR complex	k_1 (min^{-1})	k_2 (min^{-1})
Fe_2hTF–sTFR[a]	5.5 ± 0.9 (k_C)	1.4 ± 0.2 (k_N)
$Fe_2hTF_{(OX)}$–sTFR	0.6 ± 0.1	0.6 ± 0.1
Fe_NhTF–sTFR[a]	22.0 ± 0.7	1.7 ± 0.6 (k_N)
$Fe_NhTF_{(OX)}$–sTFR	–	0.6 ± 0.01
Fe_ChTF–sTFR[a]	20.6 ± 1.2	7.2 ± 0.4 (k_C)
$Fe_ChTF_{(OX)}$–sTFR	22.8 ± 10.9	0.6 ± 0.1

[a]From ref 36. See Figure S5 of the Supporting Information for iron-dependent changes as a function of time and the fit of this kinetic data to yield the rate constants in this table.

Displacement of the Synergistic Anion from Fe_2hTF. The ability of one synergistic anion (carbonate or oxalate) to displace the other from Fe_2hTF under physiologic conditions was evaluated using urea gel analysis because (as clearly shown above) CO_3^{2-}- and $C_2O_4^{2-}$-containing hTF are easily distinguished by this method. Even at relatively high (not physiologically relevant) oxalate concentrations (50 μM), CO_3^{2-} was not displaced from Fe_2hTF (Figure 3). Likewise, carbonate was unable to displace oxalate as the synergistic anion of Fe_2hTF even in the absence of added oxalate (0 μM $C_2O_4^{2-}$) (Figure 4). These results suggest that once bound to hTF, one synergistic anion (carbonate or oxalate) cannot displace the other (at least in the absence of other factors that are perhaps present in the blood). This statement appears to hold true not only at physiologically relevant normal oxalate concentrations but also at significantly elevated concentrations of oxalate, much higher than those observed in children with ASD.

ApohTF Synergistic Anion Competition. The ability of one synergistic anion (carbonate or oxalate) to compete with the other for concomitant binding with Fe^{3+} to apohTF was also assessed by a urea gel. As shown in Figure 5, when apohTF is exposed to a mixture of carbonate and oxalate at varying concentrations in the presence of an available iron source, Fe-NTA, carbonate appears to be the preferred synergistic anion for both lobes of hTF. These results suggest that, even at a very high concentration (50 μM) of oxalate, the much higher concentrations of carbonate present in the blood (20−30 mM)[46] would probably preclude the formation of $hTF_{(OX)}$.

Evaluation of the hTF Complexes by ESI-MS. Binding of oxalate to hTF was also examined by ESI-MS under nearly native conditions allowing the bound iron and synergistic anion to be observed directly.[47] On the basis of mass differences, a

dx.doi.org/10.1021/bi401190m | Biochemistry 2013, 52, 8333−8341

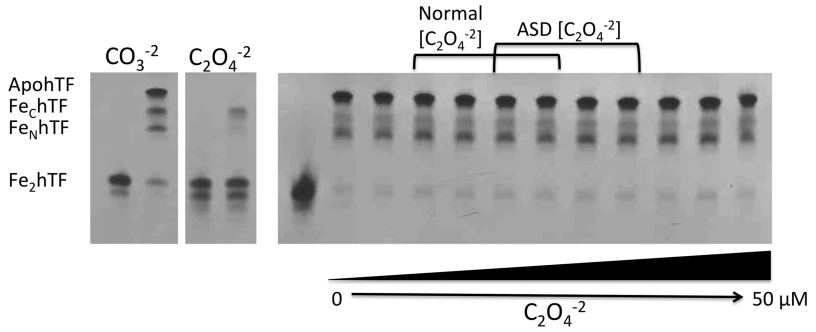

Figure 3. Displacement of carbonate (CO_3^{2-}) from Fe_2hTF by oxalate ($C_2O_4^{2-}$). Carbonate-bound Fe_2hTF was incubated at normal CO_3^{2-} concentrations (25 mM $NH_3HCO_3^{2-}$)[46] with increasing concentrations of $C_2O_4^{2-}$ ranging from normal $C_2O_4^{2-}$ concentrations (1.8−4.7 μM)[7] to ASD $C_2O_4^{2-}$ concentrations (3.5−7.5 μM)[7] and above (lanes 2−12 contained 0, 1.0, 1.8, 2.5, 3.5, 4.7, 5.6, 7.5, 10, 25, and 50 μM $C_2O_4^{2-}$, respectively). Samples were removed and electrophoresed following incubation with iron removal buffer [100 mM MES (pH 5.6) containing 300 mM KCl and 4 mM EDTA] for 15 min. The control carbonate (CO_3^{2-})- and oxalate ($C_2O_4^{2-}$)-containing Fe_2hTF samples from Figure 1A are shown at the left as a reference.

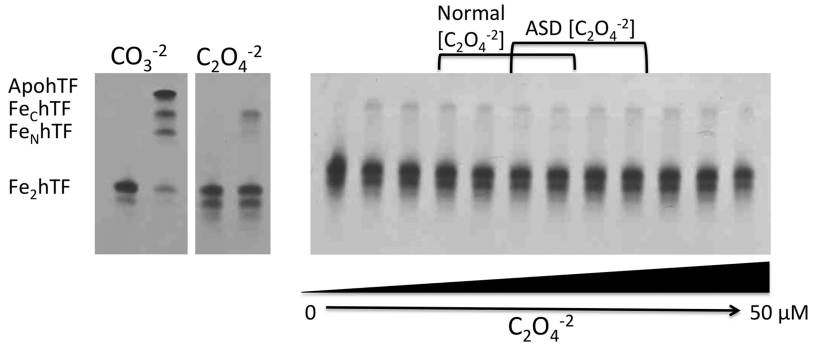

Figure 4. Displacement of oxalate ($C_2O_4^{2-}$) from Fe_2hTF by carbonate (CO_3^{2-}). Oxalate-bound Fe_2hTF was incubated at a normal serum CO_3^{2-} concentration (25 mM $NH_3HCO_3^{2-}$)[46] with increasing concentrations of $C_2O_4^{2-}$ ranging from normal $C_2O_4^{2-}$ concentrations (1.8−4.7 μM)[7] to ASD $C_2O_4^{2-}$ concentrations (3.5−7.5 μM)[7] and above (lanes 2−12 contained 0, 1.0, 1.8, 2.5, 3.5, 4.7, 5.6, 7.5, 10, 25, and 50 μM $C_2O_4^{2-}$, respectively). Samples were removed and electrophoresed following incubation with iron removal buffer [100 mM MES (pH 5.6) containing 300 mM KCl and 4 mM EDTA] for 15 min. The control carbonate (CO_3^{2-})- and oxalate ($C_2O_4^{2-}$)-containing Fe_2hTF samples from Figure 1A are shown at the left as a reference.

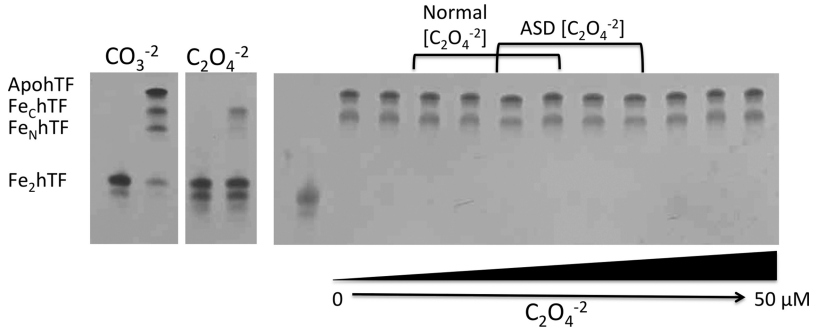

Figure 5. Synergistic anion competition for binding to apohTF. ApohTF was incubated in 25 mM (CO_3^{2-}) with increasing concentrations of $C_2O_4^{2-}$ ranging from normal $C_2O_4^{2-}$ concentrations (1.8−4.7 μM)[7] to ASD $C_2O_4^{2-}$ concentrations (3.5−7.5 μM)[7] and above (lanes 2−12 contained 0, 1.0, 1.8, 2.5, 3.5, 4.7, 5.6, 7.5, 10, 25, and 50 μM $C_2O_4^{2-}$, respectively) in the presence of excess Fe^{3+}. Samples were removed and electrophoresed following incubation with iron removal buffer [100 mM MES (pH 5.6) containing 300 mM KCl and 4 mM EDTA] for 15 min. The control carbonate (CO_3^{2-})- and oxalate ($C_2O_4^{2-}$)-containing Fe_2hTF samples from Figure 1A are shown at the left as a reference.

distinction can be made between the oxalate- and carbonate-bound forms of hTF. Additionally, acidifying the sample typically allows the simultaneous displacement of both the iron and the synergistic anion from each lobe of hTF. Of interest, we found that simple buffer exchange into the pH 5.6 oxalate buffer was not effective at replacing all carbonate (particularly in the C-lobe). Residual carbonate was clearly observed in the $Fe_ChTF_{(OX)}$ and $Fe_2hTF_{(OX)}$ samples, but not in the $Fe_NhTF_{(OX)}$ sample, suggesting that carbonate in the C-lobe was not as readily displaced (Figure S3 of the Supporting Information). This result appears to be consistent with the higher affinity of the C-lobe of hTF for iron.[21,36] In contrast, only the oxalate-bound form was observed when iron was removed prior to the buffer exchange to replace carbonate (Figure 6). The strong binding affinity of iron and/or oxalate in the C-lobe was also evident upon acidification of the sample to

dx.doi.org/10.1021/bi401190m | *Biochemistry* 2013, 52, 8333−8341

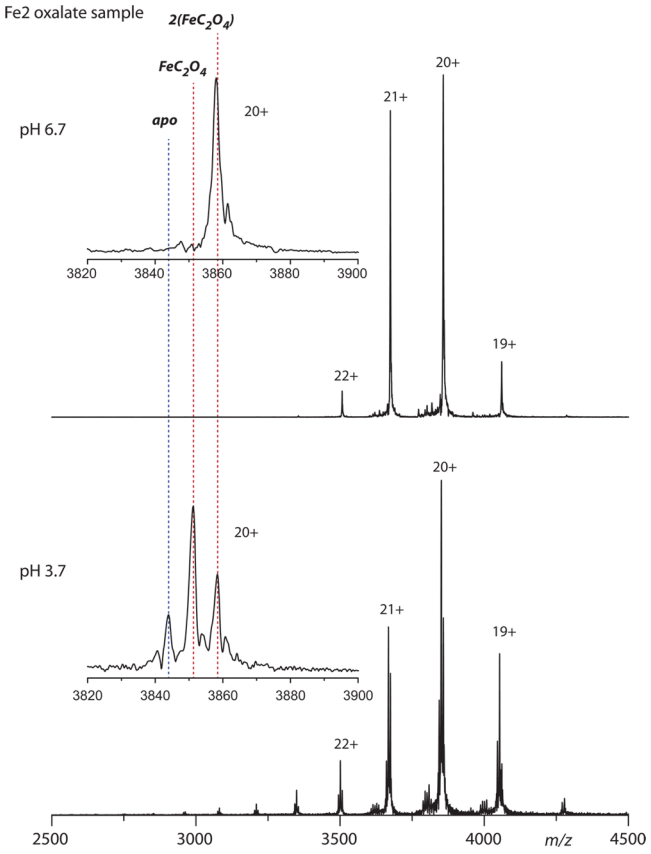

Figure 6. ESI-MS analysis of oxalate-bound forms of hTF. Spectra for hTF and each monoferric variant (Fe_C and Fe_N) were recorded at pH 6.7 and then at pH 3.7. Oxalate binding is demonstrated in the close-up of each +20 charge state (insets); theoretically calculated positions for the various ligand-bound states are labeled.

pH 3.7. Despite using a pH well below that reported for the endosome to facilitate formation of the apo species, a significant fraction of Fe_2hTF retained iron and oxalate.

Uptake of Iron and Its Circulation within the Body: Loading of hTF with Iron. A small amount of iron (~2−3 mg) enters the body daily through uptake by the enterocytes lining the intestine. The remainder of the iron that enters the circulation comes from reticuloendothelial macrophages that recycle iron from senescent erythrocytes. Thus, ~30 mg of iron is recovered and recycled each day to produce hemoglobin in reticulocytes.[20] The redox pair, Fe^{2+} and Fe^{3+}, undergoes a series of oxidations and reductions to allow their transport through cells, across cell membranes, and around the circulatory system (as Fe^{3+} within each cleft of hTF). A number of proteins are engaged in the interconversion, including ceruloplasmin and hephastin for oxidation and the cytochrome *b* ferrireductase, Dcytb, for reduction.[20] Although a good deal is known, some crucial details have yet to be elucidated, including the precise location of the loading, i.e., within a cell, at the cell surface, or both? Thus, if the local levels of oxalate at the sites of iron loading are high or the pH is low, the possibility of oxalate entering the binding cleft of hTF certainly exists.

In this work, we have endeavored to investigate the potential link between high plasma oxalate levels and iron deficiency in children with ASD. Using techniques that have been developed and validated in our laboratory, we have been able to confirm previous findings that hTF with oxalate bound as the synergistic anion [$hTF_{(OX)}$] releases far less Fe^{3+} at pH 5.6 than hTF in which carbonate serves as the synergistic anion. This finding holds true in the absence and presence of the sTFR and is significant because our previous work showed that the sTFR overwhelms and in fact trumps other contributions to the mechanism of iron release, including variations in both pH and salt.[35,36] Moreover, perhaps on the basis of our overly simple *in vitro* system, oxalate (even at pathologically relevant concentrations) appears to be unable to displace or compete with carbonate for binding of the synergistic anion to hTF. Therefore, we must conclude that it is unlikely that high oxalate concentrations promoting the formation of $hTF_{(OX)}$ are responsible for iron-refractory ID/IDA in children with ASD. Obviously, further studies are required to validate these findings *in vivo*. Finally, as previously suggested,[48] the very slow rate of release of iron from $hTF_{(OX)}$−sTFR complexes could increase the dwell times of these complexes within endocytic compartments of cells, potentially making $hTF_{(OX)}$ an effective carrier for targeted drug delivery.

■ ASSOCIATED CONTENT

Supporting Information

Kinetic constants for locked Fe_2hTF constructs in the absence and presence of the sTFR (Tables S1 and S2, respectively), urea gels for doubly locked Fe_2hTF constructs in the absence and presence of the sTFR (Figures S1 and S2, respectively), ESI-MS analysis of Fe_2hTF and the two monoferric hTF constructs showing incomplete exchange of the synergistic anions oxalate and carbonate (Figure S3), and kinetic curves and fits for the oxalate complexes of Fe_2hTF and the two monoferric hTF constructs in the absence and presence of the sTFR (Figures S4 and S5, respectively). This material is available free of charge via the Internet at http://pubs.acs.org.

■ AUTHOR INFORMATION

Corresponding Author

*Department of Biochemistry, University of Vermont, Burlington, VT 05405. E-mail: anne.mason@uvm.edu. Telephone: (802) 656-0343. Fax: (802) 862-8229.

Present Address

§A.N.L. (previously Ashley N. Steere): New England Biolabs, 240 County Rd., Ipswich, MA 01938.

Funding

This work was supported by National Institutes of Health Grants R01 DK 21739 (to A.B.M.) and R01GM061666 (to I.A.K.). A.N.L. was funded by an AHA Predoctoral Fellowship (10PRE4200010). Acquisition of an FT transform ICR mass spectrometer was supported by National Science Foundation Grant CHE-0923329 (through the Major Research Instrumentation program).

Notes

The authors declare no competing financial interest.

■ ABBREVIATIONS

ASD, autism spectrum disorders; hTF, human serum transferrin; TFR, transferrin receptor; apohTF, iron-free hTF; Fe_2hTF, recombinant N-terminal hexa-His-tagged nonglycosylated diferric hTF; Fe_NhTF, recombinant N-terminal hexa-His-tagged nonglycosylated monoferric hTF that binds iron only in the N-lobe (Y426F and Y517F mutations prevent iron from binding in the C-lobe); Fe_ChTF, recombinant N-terminal hexa-His-tagged nonglycosylated monoferric hTF that binds iron

only in the C-lobe (Y95F and Y188F mutations prevent iron from binding in the N-lobe); $Lock_N$ and $Lock_C$hTF, constructs in which both lobes are unable to release iron because of the K206E substitution in the N-lobe and the K534E, K534A, R632E, or R632A substitution in the C-lobe, respectively; $hTF_{(OX)}$, human serum transferrin with oxalate in place of carbonate as the synergistic anion; $hTF/2N_{(OX)}$, N-lobe of hTF with oxalate as the synergistic anion; sTFR, glycosylated N-terminal hexa-His-tagged soluble recombinant transferrin receptor (residues 121−760); BHK, baby hamster kidney; NTA, nitrilotriacetic acid; EDTA, ethylenediaminetetraacetic acid; TBE, tris(hydroxymethyl)aminomethane−borate−EDTA; ESI-MS, electrospray mass spectrometry.

REFERENCES

(1) Centers for Disease Control and Prevention (2012) Prevalence of Autism Spectrum Disorders: Autism and Developmental Disabilities Monitoring Network, 14 Sites, United States, 2008. *Morbidity and Mortality Weekly Report 61*, 1−19.

(2) Liu, J., Nyholt, D. R., Magnussen, P., Parano, E., Pavone, P., Geschwind, D., Lord, C., Iversen, P., Hoh, J., Ott, J., and Gilliam, T. C. (2001) A genomewide screen for autism susceptibility loci. *Am. J. Hum. Genet. 69*, 327−340.

(3) Volkmar, F. R., and Pauls, D. (2003) Autism. *Lancet 362*, 1133−1141.

(4) Kim, S. J., Brune, C. W., Kistner, E. O., Christian, S. L., Courchesne, E. H., Cox, N. J., and Cook, E. H. (2008) Transmission disequilibrium testing of the chromosome 15q11-q13 region in autism. *Am. J. Med. Genet., Part B 147B*, 1116−1125.

(5) Duchan, E., and Patel, D. R. (2012) Epidemiology of autism spectrum disorders. *Pediatr. Clin. North Am. 59*, 27−43 , ix−x.

(6) Jyonouchi, H. (2009) Food allergy and autism spectrum disorders: Is there a link? *Curr. Allergy Asthma Rep. 9*, 194−201.

(7) Konstantynowicz, J., Porowski, T., Zoch-Zwierz, W., Wasilewska, J., Kadziela-Olech, H., Kulak, W., Owens, S. C., Piotrowska-Jastrzebska, J., and Kaczmarski, M. (2012) A potential pathogenic role of oxalate in autism. *European Journal of Paediatric Neurology 16*, 485−491.

(8) Holmes, R. P., and Assimos, D. G. (1998) Glyoxylate synthesis, and its modulation and influence on oxalate synthesis. *J. Urol. 160*, 1617−1624.

(9) Linster, C. L., and Van Schaftingen, E. (2007) Vitamin C. Biosynthesis, recycling and degradation in mammals. *FEBS J. 274*, 1−22.

(10) Latif, A., Heinz, P., and Cook, R. (2002) Iron deficiency in autism and Asperger syndrome. *Autism: International Journal of Research and Practice 6*, 103−114.

(11) Dosman, C. F., Drmic, I. E., Brian, J. A., Senthilselvan, A., Harford, M., Smith, R., and Roberts, S. W. (2006) Ferritin as an indicator of suspected iron deficiency in children with autism spectrum disorder: Prevalence of low serum ferritin concentration. *Development Medicine and Child Neurology 48*, 1008−1009.

(12) Bilgic, A., Gurkan, K., Turkoglu, S., Akca, O. F., Kilic, B. G., and Uslu, R. (2010) Iron Deficiency in Preschool Children with Autistic Spectrum Disorders. *Research in Autism Spectrum Disorders 4*, 639−644.

(13) Herguner, S., Kelesoglu, F. M., Tanidir, C., and Copur, M. (2012) Ferritin and iron levels in children with autistic disorder. *Eur. J. Pediatr. 171*, 143−146.

(14) Reynolds, A., Krebs, N. F., Stewart, P. A., Austin, H., Johnson, S. L., Withrow, N., Molloy, C., James, S. J., Johnson, C., Clemons, T., Schmidt, B., and Hyman, S. L. (2012) Iron Status in Children With Autism Spectrum Disorder. *Pediatrics 130*, S154−S159.

(15) Dosman, C. F., Drmic, I. E., Brian, J. A., Harford, M., Sharieff, W., Smith, R., Moldofsky, H., Zlotkin, S., and Roberts, W. (2004) Response to Iron Supplementation in Children with Autism Spectrum Disorders. Canadian Paediatric Society's 81st Annual Meeting, Montreal, QC.

(16) Aisen, P., Enns, C., and Wessling-Resnick, M. (2001) Chemistry and biology of eukaryotic iron metabolism. *Int. J. Biochem. Cell Biol. 33*, 940−959.

(17) Lozoff, B., and Georgieff, M. K. (2006) Iron Deficiency and Brain Development. *Seminars in Pediatric Neurology 13*, 158−165.

(18) Lukowski, A. F., Koss, M., Burden, M. J., Jonides, J., Nelson, C. A., Kaciroti, N., Jimenez, E., and Lozoff, B. (2010) Iron deficiency in infancy and neurocognitive functioning at 19 years: Evidence of long-term deficits in executive function and recognition memory. *Nutr. Neurosci. 13*, 54−70.

(19) Acikyol, B., Graham, R. M., Trinder, D., House, M. J., Olynyk, J. K., Scott, R. J., Milward, E. A., and Johnstone, D. M. (2013) Brain transcriptome perturbations in the transferrin receptor 2 mutant mouse support the case for brain changes in iron loading disorders, including effects relating to long-term depression and long-term potentiation. *Neuroscience 235*, 119−128.

(20) Sheftel, A. D., Mason, A. B., and Ponka, P. (2011) The long history of iron in the universe and in health and disease. *Biochim. Biophys. Acta 1820*, 161−187.

(21) Aisen, P., Leibman, A., and Zweier, J. (1978) Stoichiometric and site characteristics of the binding of iron to human transferrin. *J. Biol. Chem. 253*, 1930−1937.

(22) Schade, A. L., Reinhart, R. W., and Levy, H. (1949) Carbon dioxide and oxygen in complex formation with iron and siderophilin, the iron-binding component of human plasma. *Arch. Biochem. 20*, 170−172.

(23) MacGillivray, R. T., Moore, S. A., Chen, J., Anderson, B. F., Baker, H., Luo, Y., Bewley, M., Smith, C. A., Murphy, M. E., Wang, Y., Mason, A. B., Woodworth, R. C., Brayer, G. D., and Baker, E. N. (1998) Two high-resolution crystal structures of the recombinant N-lobe of human transferrin reveal a structural change implicated in iron release. *Biochemistry 37*, 7919−7928.

(24) Price, E. M., and Gibson, J. F. (1972) A re-interpretation of bicarbonate-free ferric transferrin E.P.R. spectra. *Biochem. Biophys. Res. Commun. 46*, 646−651.

(25) Shaw, D. E., Maragakis, P., Lindorff-Larsen, K., Piana, S., Dror, R. O., Eastwood, M. P., Bank, J. A., Jumper, J. M., Salmon, J. K., Shan, Y., and Wriggers, W. (2010) Atomic-Level Characterization of the Structural Dynamics of Proteins. *Science 330*, 341−346.

(26) Gerstein, M., Anderson, B. F., Norris, G. E., Baker, E. N., Lesk, A. M., and Chothia, C. (1993) Domain closure in lactoferrin. Two hinges produce a see-saw motion between alternative close-packed interfaces. *J. Mol. Biol. 234*, 357−372.

(27) Gaber, B. P., Miskowski, V., and Spiro, T. G. (1974) Resonance Raman scattering from iron(III)- and copper(II)-transferrin and an iron(III) model compound. A spectroscopic interpretation of the transferrin binding site. *J. Am. Chem. Soc. 96*, 6868−6873.

(28) Lin, L. N., Mason, A. B., Woodworth, R. C., and Brandts, J. F. (1993) Calorimetric studies of the binding of ferric ions to human serum transferrin. *Biochemistry 32*, 9398−9406.

(29) Morgan, E. H., and Appleton, T. C. (1969) Autoradiographic localization of 125-I-labelled transferrin in rabbit reticulocytes. *Nature 223*, 1371−1372.

(30) Morgan, E. H. (1981) Inhibition of reticulocyte iron uptake by NH_4Cl and CH_3NH_2. *Biochim. Biophys. Acta 642*, 119−134.

(31) He, Q. Y., Mason, A. B., Tam, B. M., MacGillivray, R. T., and Woodworth, R. C. (1999) Dual role of Lys206-Lys296 interaction in human transferrin N-lobe: Iron-release trigger and anion-binding site. *Biochemistry 38*, 9704−9711.

(32) Halbrooks, P. J., He, Q. Y., Briggs, S. K., Everse, S. J., Smith, V. C., MacGillivray, R. T., and Mason, A. B. (2003) Investigation of the mechanism of iron release from the C-lobe of human serum transferrin: Mutational analysis of the role of a pH sensitive triad. *Biochemistry 42*, 3701−3707.

(33) Halbrooks, P. J., Giannetti, A. M., Klein, J. S., Bjorkman, P. J., Larouche, J. R., Smith, V. C., MacGillivray, R. T., Everse, S. J., and Mason, A. B. (2005) Composition of pH-sensitive triad in C-lobe of

human serum transferrin. Comparison to sequences of ovotransferrin and lactoferrin provides insight into functional differences in iron release. *Biochemistry 44*, 15451−15460.
(34) Dewan, J. C., Mikami, B., Hirose, M., and Sacchettini, J. C. (1993) Structural evidence for a pH-sensitive dilysine trigger in the hen ovotransferrin N-lobe: Implications for transferrin iron release. *Biochemistry 32*, 11963−11968.
(35) Steere, A. N., Byrne, S. L., Chasteen, N. D., and Mason, A. B. (2012) Kinetics of iron release from transferrin bound to the transferrin receptor at endosomal pH. *Biochim. Biophys. Acta 1820*, 326−333.
(36) Byrne, S. L., Chasteen, N. D., Steere, A. N., and Mason, A. B. (2010) The unique kinetics of iron-release from transferrin: The role of receptor, lobe-lobe interactions and salt at endosomal pH. *J. Mol. Biol. 396*, 130−140.
(37) Schlabach, M. R., and Bates, G. W. (1975) The synergistic binding of anions and Fe^{3+} by transferrin. Implications for the interlocking sites hypothesis. *J. Biol. Chem. 250*, 2182−2188.
(38) Halbrooks, P. J., Mason, A. B., Adams, T. E., Briggs, S. K., and Everse, S. J. (2004) The oxalate effect on release of iron from human serum transferrin explained. *J. Mol. Biol. 339*, 217−226.
(39) Mason, A. B., He, Q. Y., Halbrooks, P. J., Everse, S. J., Gumerov, D. R., Kaltashov, I. A., Smith, V. C., Hewitt, J., and MacGillivray, R. T. (2002) Differential effect of a his tag at the N- and C-termini: Functional studies with recombinant human serum transferrin. *Biochemistry 41*, 9448−9454.
(40) Byrne, S. L., Leverence, R., Klein, J. S., Giannetti, A. M., Smith, V. C., MacGillivray, R. T., Kaltashov, I. A., and Mason, A. B. (2006) Effect of glycosylation on the function of a soluble, recombinant form of the transferrin receptor. *Biochemistry 45*, 6663−6673.
(41) Steere, A. N., Byrne, S. L., Chasteen, N. D., Smith, V. C., MacGillivray, R. T., and Mason, A. B. (2010) Evidence that His349 acts as a pH-inducible switch to accelerate receptor-mediated iron release from the C-lobe of human transferrin. *JBIC, J. Biol. Inorg. Chem. 15*, 1341−1352.
(42) Byrne, S. L., and Mason, A. B. (2009) Human serum transferrin: A tale of two lobes. Urea gel and steady state fluorescence analysis of recombinant transferrins as a function of pH, time, and the soluble portion of the transferrin receptor. *JBIC, J. Biol. Inorg. Chem. 14*, 771−781.
(43) Byrne, S. L., Steere, A. N., Chasteen, N. D., and Mason, A. B. (2010) Identification of a kinetically significant anion binding (KISAB) site in the N-lobe of human serum transferrin. *Biochemistry 49*, 4200−4207.
(44) Eckenroth, B. E., Steere, A. N., Chasteen, N. D., Everse, S. J., and Mason, A. B. (2011) How the binding of human transferrin primes the transferrin receptor potentiating iron release at endosomal pH. *Proc. Natl. Acad. Sci. U.S.A. 108*, 13089−13094.
(45) Steere, A. N., Chasteen, N. D., Miller, B. F., Smith, V. C., Macgillivray, R. T., and Mason, A. B. (2012) Structure-Based Mutagenesis Reveals Critical Residues in the Transferrin Receptor Participating in the Mechanism of pH-Induced Release of Iron from Human Serum Transferrin. *Biochemistry 51*, 2113−2121.
(46) Raphael, K. L., Wei, G., Baird, B. C., Greene, T., and Beddhu, S. (2011) Higher serum bicarbonate levels within the normal range are associated with better survival and renal outcomes in African Americans. *Kidney Int. 79*, 356−362.
(47) Kaltashov, I. A., Bobst, C. E., Zhang, M., Leverence, R., and Gumerov, D. R. (2012) Transferrin as a model system for method development to study structure, dynamics and interactions of metalloproteins using mass spectrometry. *Biochim. Biophys. Acta 1820*, 417−426.
(48) Yoon, D. J., Chu, D. S., Ng, C. W., Pham, E. A., Mason, A. B., Hudson, D. M., Smith, V. C., MacGillivray, R. T., and Kamei, D. T. (2009) Genetically engineering transferrin to improve its in vitro ability to deliver cytotoxins. *J. Controlled Release 133*, 178−184.